J. Synchrotron Rad. (1998). **5**, 434–436

Design of a 2 T multipole wiggler insertion device for the SRS

James A. Clarke,* Neil Bliss, David Bradshaw, Cheryl Dawson, Barry Fell, Neville Harris, Gary Hayes, Michael Poole and Ron Reid

CLRC Daresbury Laboratory, Warrington WA4 4AD, UK. E-mail: j.a.clarke@dl.ac.uk

(*Received 4 August 1997; accepted 6 November 1997*)

Two new identical insertion devices have been designed for the Daresbury SRS. They are 2 T permanent-magnet multipole wigglers that will provide high flux in the X-ray region. This paper describes the magnetic and mechanical design of the arrays of steel pole pieces and permanent-magnet blocks. Also given is the engineering design of the support structure that will cope with the very large forces present while maintaining high levels of precision in gap setting and parallelism. The engineering design has been fully assessed using finite-element techniques to predict the deflections of critical parts of the structure. These two devices are due to be installed into the SRS by the end of 1998.

Keywords: insertion devices; multipole wigglers; permanent magnets.

1. SRS upgrade

A major upgrade to the Daresbury SRS that will enhance the facility for its users has recently been approved. A major rearrangement of the components in the storage ring allows for the inclusion of two more insertion devices (Clarke & Poole, 1996). These devices will provide powerful X-rays for two new beamlines, with up to two stations per beamline. The insertion devices are identical and have been specified to provide the maximum flux possible at about 10 keV. The straight length available in the second-generation SRS is just over 1 m so it is difficult to build a device with many poles. The chosen design has nine 2 T poles with two 1.8 T end poles. This provides a very powerful source with about four times more photons at 10 keV than the present superconducting 6 T wavelength shifter and about 25 times more than a standard dipole source (Fig. 1). The multipole wigglers are due to be installed into the SRS by the end of 1998 with the beamline commissioning complete by the end of 1999.

2. Magnetic design

The peak magnetic field for the multipole wigglers was chosen to be 2 T because this provides a high critical energy of 5.3 keV and also sufficient horizontal angular deflection of the electron beam (about 15 mrad) to satisfy two experimental stations. The number of poles that can be fitted into the straight section available is very dependent upon the magnet pole gap.

Extensive accelerator-physics time was spent examining the vertical aperture in the storage ring. Beam scrapers were used to assess the effect of a restricted aperture on the beam lifetime, injection and energy ramp. This work concluded that the beam stay clear of 36 mm could be reduced to a much more aggressive 15 mm without reducing the stored beam lifetime by more than about 15% (Clarke & Owen, 1996). The vacuum-chamber design was studied in detail to ensure the most efficient magnet design possible. This optimization resulted in the vacuum chamber having strengthening ribs at several points on the outside of the vessel so that the vessel thickness and therefore the gap between the pole pieces could be kept to a minimum. Furthermore, the vacuum chamber material was chosen to be titanium instead of stainless steel mainly because of the much reduced weld distortion. The final vacuum vessel design (Fig. 2) has a material thickness of 1.0 mm at the pole pieces and this is increased to 4 mm for the strengthening ribs, which are under the permanent-magnet pieces. Allowance for geometric tolerances and clearance between the vessel and the poles leads to a magnet gap of 19.2 mm between the steel pole pieces, with the permanent-magnet material gap increased to 27.2 mm to allow room for the strengthening ribs. The design also includes vertical electron beam-position monitors at either end to ensure that the beam passes centrally through the vessel. A prototype vessel has now been successfully manufactured that meets this magnet gap specification. Full details of the prototype vessel dimensions and achieved tolerances are given by Bliss & Dawson (1997).

An assessment was made of the period of the multipole wiggler required to meet 2 T with a gap of 19.2 mm. It was found that an electromagnet solution was possible though with a much longer period than for the permanent-magnet hybrid solution. A period of 200 mm was chosen for the permanent-magnet hybrid multipole wiggler. This is a challenging but feasible target. This chosen period then allows for nine full poles with room for two end poles to correctly terminate the device.

Much of the magnet design was performed with two-dimensional models using *Opera-2D* (Vector Fields) and *Pandira* (Billen & Young, 1996); good agreement was found with these two codes. However, the two-dimensional model was inadequate for determining the optimum width of the pole and permanent magnet pieces. This optimization was carried out with a fully three-dimensional model using *Opera-3D* running the magnetostatic code *Tosca* (Vector Fields). These three-dimensional models suggested that the permanent-magnet material should extend horizontally beyond the steel poles, as well as vertically, for the most efficient solution. Furthermore, additional permanent-magnet pieces were placed at the sides of the steel poles to reduce the flux leakage in the horizontal direction (Clarke, 1997).

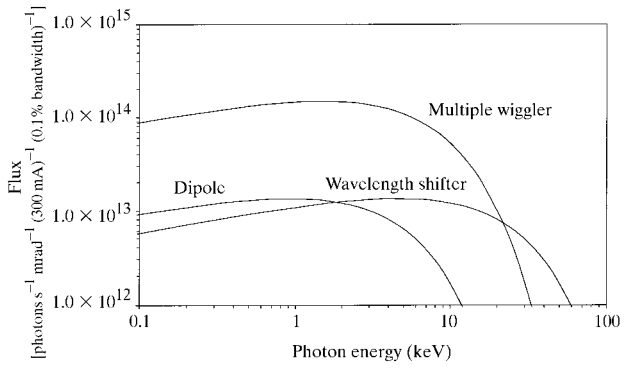

Figure 1
Flux comparison between the SRS dipoles, 6 T wavelength shifter and multipole wiggler.

Table 1
Parameter list for the multipole wiggler.

PM = permanent magnet.

Peak field on axis	2 T
Minimum gap	19.2 mm
Period	200 mm
K value	37.4
Number of full-strength poles	9
Pole material	Vanadium permendur
PM material	NdFeB
Assumed remanent field	1.35 T
Pole dimensions	100 × 80 × 30 mm
Main PM-block dimensions	130 × 120 × 70 mm
Side PM-block dimensions	96 × 10 × 30 mm
Total length of magnet	1.078 m
Gap setting accuracy	<10 μm
Gap resolution	<5 μm
Parallelism of two arrays	<±40 μm
Force at minimum gap	50 kN
Trim coil ampere turns	450 At

Since the multipole wiggler contains only nine full-strength poles it was realized that the end poles could make a significant contribution to the photon flux emitted. To maximize the end-pole contribution they were designed to have as high a field as possible while still terminating the magnet correctly. Again, two-dimensional models were used to assess the possibilities but the final optimization was carried out in three dimensions. The optimum end design was found to have a field level of about 1.8 T. The end has a reduced-length pole piece and no permanent-magnet side pieces. A simple trim coil is wound around the whole magnet to ensure that there is no net angle and displacement of the electron beam. A full magnet parameter list is given in Table 1. A view of one complete array is given in Fig. 3.

3. Engineering design

3.1. *Magnet arrays*

Each magnet array is built up from a series of sub-assemblies; these consist of a permanent-magnet block or steel pole secured into a non-magnetic holder. The magnet blocks are bonded to their holders with epoxy resin. The steel pole pieces are further held in place with non-magnetic fasteners at their base because they have to withstand particularly large forces. An assembly fixture will be used to assemble and disassemble the magnet block and pole holders onto the support beams. The fixture will be capable of removing and replacing a single magnet block or pole assembly in the middle of the array while the remaining blocks and pole pieces are still in place. The assembled array of pole faces has a flatness tolerance of 30 μm and shims have been included between the pole holders and the support beam to ensure this specification is achievable. A gap of 0.1 mm separates each of the magnet block and pole assemblies to allow individual holders to be removed.

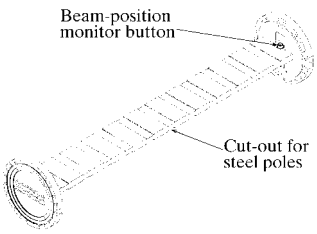

Figure 2
Sketch of the multipole wiggler vacuum vessel.

3.2. *Magnet support structure*

The magnet support structure has to cope with dramatically changing magnetic forces as the magnet gap is altered, while still maintaining a very high parallelism between the two arrays. The vertical magnetic force at the maximum gap of 200 mm is only a few hundred Newtons. As this gap is reduced, this force increases exponentially squared until, at the minimum gap, it is about 50 kN. Compensating spring assemblies, acting between the support beams and the main support structure, have been added to provide a counteracting force. Four springs are fitted to each beam with each spring providing a counteracting force of about 8 kN at the minimum magnet gap. The spring force is chosen to be sufficient to reduce the deflection of the support beams to within the magnet array parallelism tolerance while allowing the springs to be small enough to fit into the limited space available. The support structure has been modelled using finite-element analysis (FEA) to ensure that the parallelism tolerance can be met; the model was performed at the minimum magnet gap and with a design load of 60 kN (giving a 20% contingency).

The support structure is of a C-shape to enable clear access along the full length of the magnet gap. This allows the whole device to be independent of the storage-ring electron-beam vacuum chamber. Initially, a tapered A-frame design was modelled but it was found that a more symmetric upright support frame was necessary. The three-dimensional *Mechanica* (Parametric Technology Corporation) FEA model was a half-symmetry model with the plane of symmetry running vertically through the lengthwise centre of the device. Shell elements were used for the main support frame, magnet array beam and compensating spring supports. The compensating spring mechanisms and support rods were not included since they were complex to model and were not regarded as a problem area. The forces produced by the springs were simply applied as face or point loads at appropriate points. The magnet arrays were omitted and the load was applied as a uniform load along the length of the beam. The variation of force along the pole pieces was expected to make negligible difference to the distortion of the mounting face.

Fig. 4 shows an isometric view of greatly exaggerated deformations with colour contoured fringes indicating the total magnitude displacements. It is evident from the contour plot that parallelism tolerance is only significant for rotations about the azimuthal axis (the roll of the magnet arrays). Rotations about the horizontal axis (tilt of the magnet arrays), which are more important from the point of view of field uniformity, are very

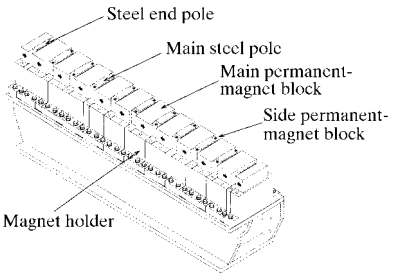

Figure 3
A complete array of the multipole wiggler. The arrows indicate the direction of magnetization.

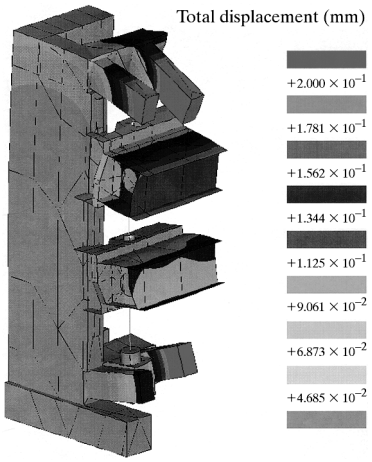

Figure 4
Calculated deformations (in mm) using FEA of half of the multipole wiggler support structure. The deformations, represented by the coloured contours, are greatly exaggerated.

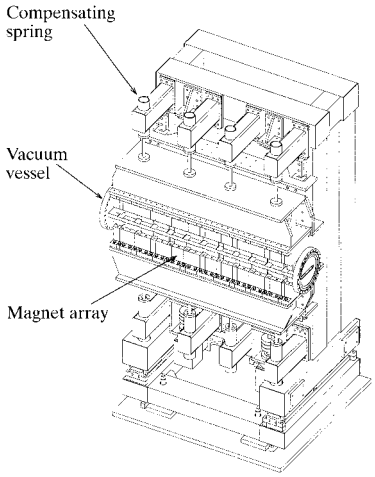

Figure 5
View of the complete multipole wiggler magnet. The device is shown at its minimum gap position with the vacuum vessel in place.

small. Parallelism roll is calculated to be 44 μm for the top array over the pole width and 35 μm for the bottom array. These values are well within the specification of ±40 μm although they do not take into account cumulative machining tolerances and other errors. The shift in nominal gap centre has also been calculated and found to be 27 μm.

3.3. *Drive system*

The drive system consists of two precision leadscrew shafts, each with a left- and right-hand thread. Two left-hand nuts are attached to the upper carriage and two right-hand nuts to the lower carriage. As the two leadscrews are rotated in synchronism the magnet gap is adjusted symmetrically about the electron beam axis. A low backlash gearbox is attached to each leadscrew *via* an extremely low backlash coupling and driven by an AC brushless motor fitted with an integral resolver and brake. The control system for adjusting the magnet gap is a closed-loop servo control with two linear encoders attached directly between the upper and lower carriages at a position close to each ballscrew. Two precision limit switches, repeatable to ±1 μm, are positioned at the minimum gap and two end-of-stroke switches are positioned at the maximum gap. Adjustable fixed stops are also incorporated in case of a limit switch failure. A torque limiter facility, to prevent damage to the mechanical drive, is also included in the control system. The magnet gap will be adjustable at a rate of 3 mm s^{-1}, which gives a minimum time to close the gap from the fully open position of 30 s.

4. Conclusions

The magnetic and engineering design for the two multipole wigglers is now complete. The final magnet design is shown in Fig. 5. The magnet design requires the use of high-specification materials and very high tolerances. These tolerances will be met by a sophisticated high-precision engineering solution that has been described here. The orders for the key components were scheduled to have been placed during the Summer of 1997, with full mechanical and magnet testing planned for the early part of 1998. The machine shutdown for installation will be later that year and the beamline will become available during 1999.

References

Billen, J. H. & Young, L. M. (1996). Los Alamos National Laboratory Report, LA-UR-96-1834. LANL, Los Alamos, NM, USA.
Bliss, N. & Dawson, C. (1997). *Proceedings of the 1997 Particle Accelerator Conference*, Vancouver. To be published.
Clarke, J. A. (1997). *Proceedings of the 1997 Particle Accelerator Conference*, Vancouver. To be published.
Clarke, J. A. & Owen, H. L. (1996). *Proceedings of the 1996 European Particle Accelerator Conference*, Sitges, pp. 620–622. Bristol: Institute of Physics.
Clarke, J. A. & Poole, M. W. (1996). *Proceedings of the 1996 European Particle Accelerator Conference*, Sitges, pp. 623–625. Bristol: Institute of Physics.